Solid Freeform Fabrication 2024: Proceedings of the 35th Annual International
Solid Freeform Fabrication Symposium – An Additive Manufacturing Conference
Reviewed Paper

In-situ print layer height correction framework for wire arc additive manufacturing

Wei Sheng Lim, Siddharth Ganesh, Gim Song Soh

Engineering Product Development, Singapore University of Technology and Design, Singapore 487372, Singapore

Abstract

Wire arc additive manufacturing (WAAM) is a form of layered manufacturing method that relies on the predictable deposition of weld beads layers upon layers to form a final part. Within a layer, utilization of variable bead width toolpath planning has been shown to produce geometrically accurate void-free shapes. However, due to the inherent variability of the WAAM process, print height deviations can still occur, causing uneven surface deposition within a layer. Without intervention, this error would stack with each layer and lead to print failure. To overcome this issue, an in-situ print height correction framework was developed. This approach utilizes a profile sensor to determine the height variation of a print layer and adjust its process to correct the height difference at the next layer toolpath using a regression-based bead-width process parameter model. An example part was printed where the standard deviation of the layer height stabilized below 1mm after 13 layers.

Introduction

Wire arc additive manufacturing (WAAM) is a form of additive manufacturing where wire-based feedstock material is deposited layer by layer using an electric arc as an energy source to print a part. Each layer is formed by depositing multiple beads following a predetermined path to cover the required area. The high deposition rate of WAAM makes it attractive to print large parts in a reasonable time frame, and these parts can require more than a hundred layers to reach the required print height. The large layer count means any deviations or inconsistencies accumulated over the layers will affect geometrical accuracy or lead to print failure. As such, developing an approach for a reliable and predictable deposition of each weld bead within and across layers is essential to prevent error accumulation, which is still an open research challenge.

Various works have been performed to reduce errors within and between layers based on improving overlapping modeling, devising toolpath and process control strategy, and incorporating in-situ intervention. To improve overlapping models, Suryakumar et al. [1] proposed a flat top model to determine the spacing between weld beads such that weld beads can be overlapped to form a flat surface for the next layer to deposit on. Subsequently, Ding et al. [2] proposed another overlap ratio based on a tangent overlap model and showed reduced error across multiple layers. However, variations in the top surface height are still noted in both approaches. Inspired by the above authors, Soh and Oh [3] proposed a varying ratio flat-top overlapping model to overcome this problem, which relies on determining an optimal overlap ratio for a particular bead geometry. Others also include the work by Hu et al. [4], where they focused on resolving the geometrical abnormalities of the hump at the start and the crater at the end of the bead. They proposed to exceed the overlap regions of the start-stop by some amount for closed-loop paths while alternating the start-stop regions for open-loop paths to minimize the height build-up.

Next, on the toolpath and process control strategy development, Wang et al. [5] proposed the use of a water-pouring rule to generate a zig-zag toolpath with a single start-stop. Such a toolpath strategy can be combined with process parameter optimization methods used by Rosli et al. [6] and Youheng et al. [7] to minimize height variation. However, the large bead width encountered in WAAM results in poor forming accuracy when the outer boundary is not aligned with the toolpath direction. Ding et al. [8] investigated contour-based adaptive width toolpath planning, and subsequently, Xiong et al. [9] integrated the approach with process planning. Such a printing strategy was found to improve from the traditional fixed width contour toolpath and can achieve high dimensional accuracy while preventing the formation of voids within the part due to under-printing. Note that voids are undesirable as they lead to poorer mechanical properties of the overall part and contribute to errors in a layer's height profile. Others also include the work by Lam et al. [10], where they focused on resolving the overhang height variation problem using a data-driven process planning approach.

Lastly, on in-situ intervention, [11], [12] utilized the milling process to create a flat top surface for the next layer to deposit on, which they term Hybrid-WAAM. Such an intervention method showed the ability to reset error accumulation to ensure continued printing with a reasonable degree of geometrical accuracy. However, any intervention strategies require additional processes, which leads to longer print time and additional material consumption, which is undesirable. To overcome this, closed-loop process control, such as that developed by Li et al. [13], can be used to control the process parameter of the next layer bead section print to correct the part's height and width error based on the measured dimension of the previous print. While it showed a great ability to control error across multiple layers, it was only suitable for simple geometry as it requires beads to be deposited directly on top of each other. This limits the control process to simple cuboid shape where there is a constant number of beads and the beads across the layers are aligned. Reinforcement learning has also been proposed by Dharmawan et al. [14] where a set of agents work together to control each segment's process parameter. The agent is trained on a data set based on fixed parameter single bead study and works together to achieve a flat top surface. While the process is promising, it was limited to a constant width process and showed large errors in the initial few layers, as attributed to the learning process. This prevents the use of adaptive bead width path planning which have been shown to be beneficial in achieving high accuracy.

It is important to note that even when choosing the right offline process parameters and suitable toolpaths, print errors will still accumulate due to WAAM's inherent process variation. As such, we propose to use a feedback loop to achieve in-situ process correction planning, leveraging a regression-based process map model. To test the feasibility of the proposed approach, a sample part requiring adaptive bead width is printed with and without bead height correction control.

WAAM In-Situ Height Correction

Fig. 1 provides an overview of the proposed WAAM in-situ height correction framework, from the planning to the printing stage. During the planning stage, a model of the desired part is first sliced based on a constant height H_c, generating the required print geometry for each layer. Next, adaptive width toolpath planning is performed on all layers to generate a database of each layer's toolpath and process parameters for each bead segment's required width. For more details,

the readers can refer to [9]. This database will subsequently be used during the printing process to extract the appropriate toolpath and process plans for printing at a particular layer height H_n. Note that H_c does not need to correspond to the expected layer thickess as the actual layer chosen is based on measurement rather than sequential order. As such, a small H_c provides a finer resolution, allowing the layer picked to be closer to the actual height during the printing process.

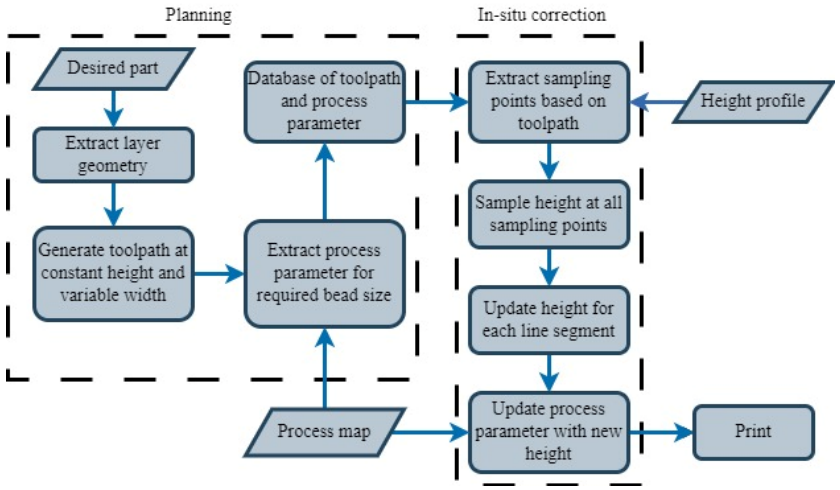

Fig. 1: Overall framework of the WAAM In-situ height correction process

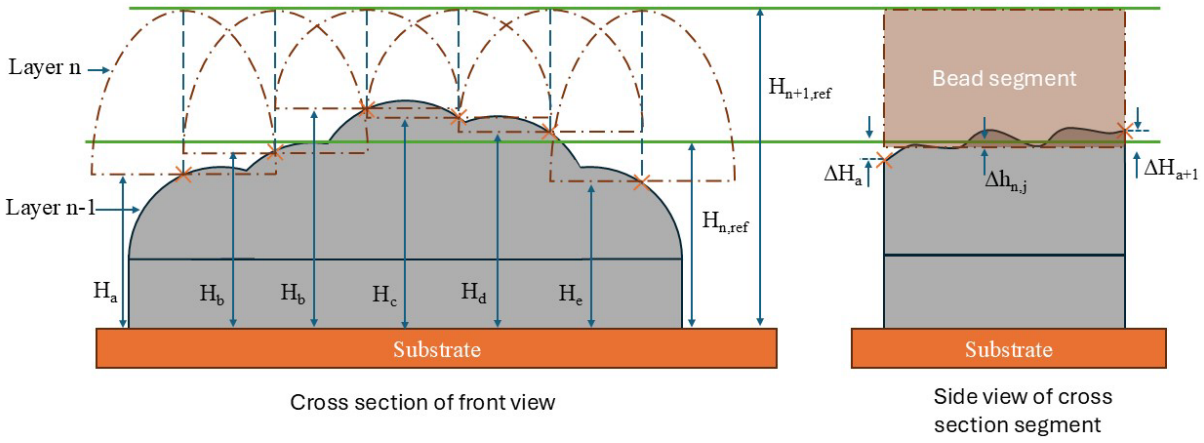

Fig. 2: Height compensation strategy

Due to WAAM's inherited process variation, the resulting print geometry at the (n-1)th layer could end up as illustrated in Fig. 2. Such height variation, if left uncorrected, would lead to print inaccuracies or print failures. To correct for such error at the nth layer, our in-situ correction methodology compares the height difference between the computed reference $H_{n,ref}$ toolpath height and printed height of the (n-1)th layer and updates the process plan of the nth layer taking into account the required compensated height profile, based on the approach described as follows.

A laser scanner first obtains the surface profile of the (n-1)th layer by scanning its top surface. For each point in the nth layer toolpath, its corresponding printed height H_i, is then sampled from the measured surface profile and its difference with respect to a reference height

determined. The reference height $H_{n,ref}$ can be found as the mean of all sampled points in the nth layer.

For each toolpath line segment j, consisting of point i and i+1, the required height compensation Δh_j is computed as the average of the error at both points, detailed in Eqn. 1.

$$\Delta h_{n,j} = 0.5\big(H_{n,ref} - H_i\big) + 0.5\big(H_{n,ref} - H_{i+1}\big) \quad (1)$$

Since there is no dependence on the previous toolpath, this correction approach is expected to work well even with complex and varying toolpaths.

To choose the appropriate process parameter to yield a desired bead geometry, a process model is needed to map the process parameters (wire feed speed v_{wire} and torch travel speed v_{torch}) to the printed bead geometry (width $w_{bead}$and height h_{bead}). To construct the process model, experiments of varying process parameters were performed to experimentally determine its influence on bead geometry. For each of these process parameters, a model is formed using multivariate regression (assuming that they are independent) using the experimental data, as denoted in Eqn. 2.

$$v_{wire} = f(w_{bead}, h_{bead}), \qquad v_{torch} = g(w_{bead}, h_{bead}) \quad (2)$$

Now, the required wire feed and torch speed can be obtained from the inverse model, using the required bead width and corrected height geometry as shown in Eqn. 3.

$$v_{wire,j} = f\big(w_j, h_c + \Delta h_j\big), \qquad v_{torch,i} = g\big(w_j, h_c + \Delta h_j\big) \quad (3)$$

Notice that, the proposed regression model enables the use of coarse intervals to explore process parameters while enabling interpolation and extrapolations to achieve finer details. This helps control the amount of experimental data required to be an acceptable amount. A rectangular window of allowable bead width and height range was chosen to ensure a consistent height adjustment range for all bead widths. The range of bead width and height is fitted such that all v_{wire} and v_{torch} within the window is kept at allowable value. This is important as the stable process parameter range is limited. Exceeding the range could result in unstable welding with poor bead formation.

Experimental setup

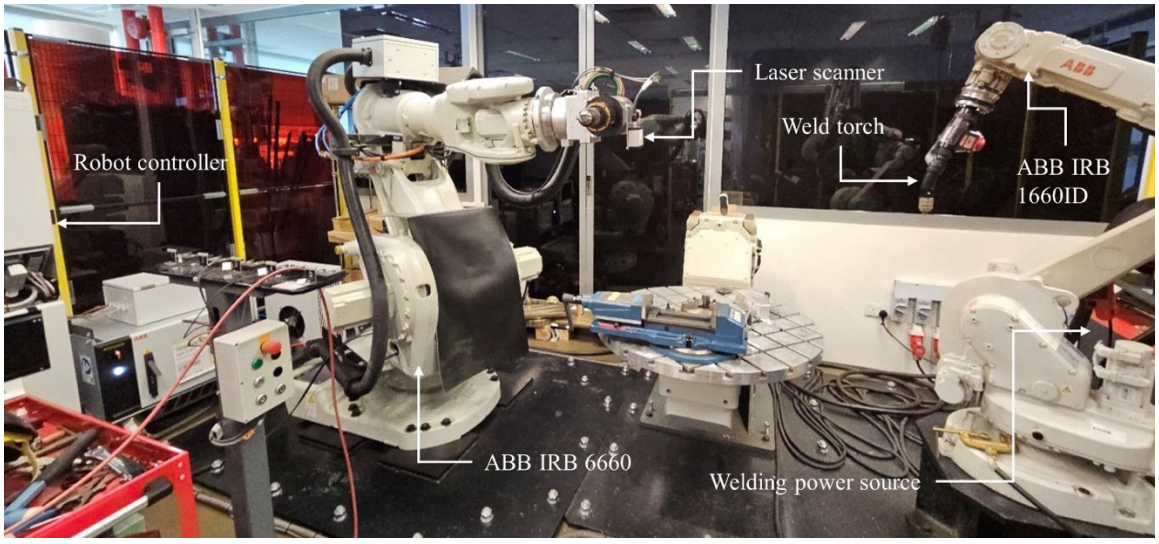

Fig. 3: Wire arc additive manufacturing set up for Experimentation

To test the print correction strategy, the cold metal transfer based WAAM setup at the Singapore University of Technology and Design, as shown in Fig. 3, was utilized. The additive capability is provided by the welding torch (Fronius WF 60i Robacta Drive) held by a robotic arm (ABB IRB 1660ID) with a welding power source (Fronius TPS 400i) powering the torch. A secondary robotic arm manipulator (ABB IRB 6660) holds a laser line scanner measurements system (Micro Epsilon scanCONTROL 3010-100/BL) to obtain a particular layer height profile.

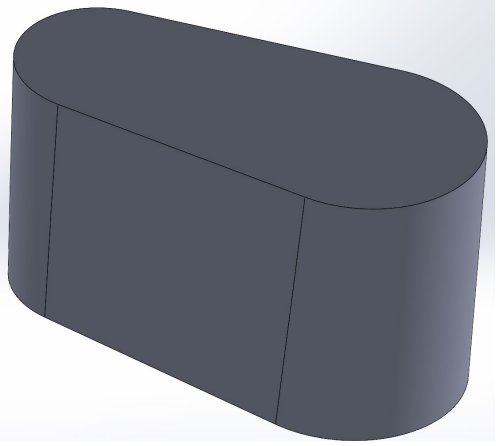

Fig. 4: Rounded bar as example geometry with varying width

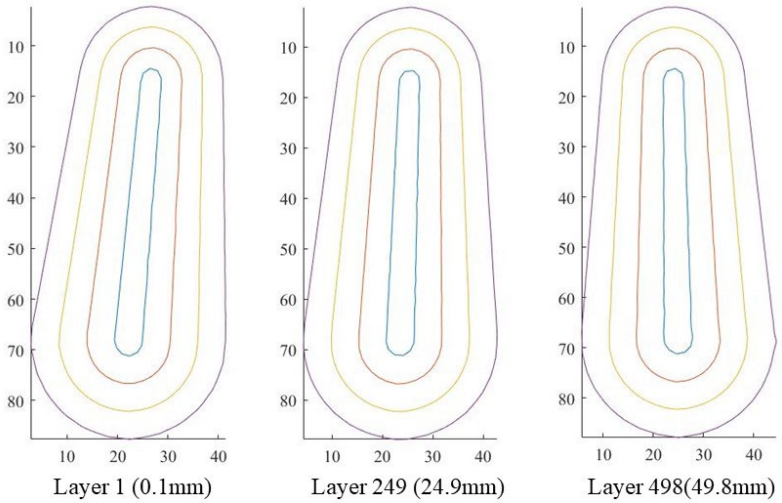

Fig. 5: Toolpath of example geometry at different layers

The experiments were conducted to test printing a 50mm tall, rounded bar with different radii at each end, as shown in Fig. 4. This geometry was chosen as an example since it requires complex planning, which involves varying bead width within the layer and varying height to adjust for height variations. The part is sliced with a layer height of 0.1mm with some example layers as shown in Fig. 5. The slight twist of the part induces minimal overhang and results in each layer having a unique path. This verifies the ability for the process the work even when the path between layers are not aligned. The material used is Nickel aluminum bronze, a common material used in marine components such as propellers, whose large size benefits from using WAAM.

Results and Discussion

A full factorial experiment was carried out with parameters detailed in Table I totaling 35 experimental values, where 100mm long beads were printed onto a flat substrate shown in Fig. 6. We then extracted the average bead width and height for each bead in the center 60mm section to remove inconsistencies from start stop regions. Notice that beads deposited with wire feed of 5 m/min and 6 m/min with higher torch speeds of 0.42 m/min and 0.6 m/min, as highlighted by the red box in Fig. 6, showed poor bead formulation and should be discarded in the process window.

Table I: Process parameter levels for single bead study

Level	Wire feed (m/min)	Torch speed(m/min)
-3	-	0.3
-2	5	0.36
-1	6	0.42
0	7	0.48
1	8	0.54
2	9	0.6
3	-	0.66

7	6	6	6	6	6	6	6	5	5	5	5	Wire (m/min)
0.66	0.3	0.36	0.42	0.48	0.54	0.6	0.66	0.3	0.36	0.42	0.54	Torch (m/min)

Fig. 6: Section of single bead study of nickel aluminium bronze

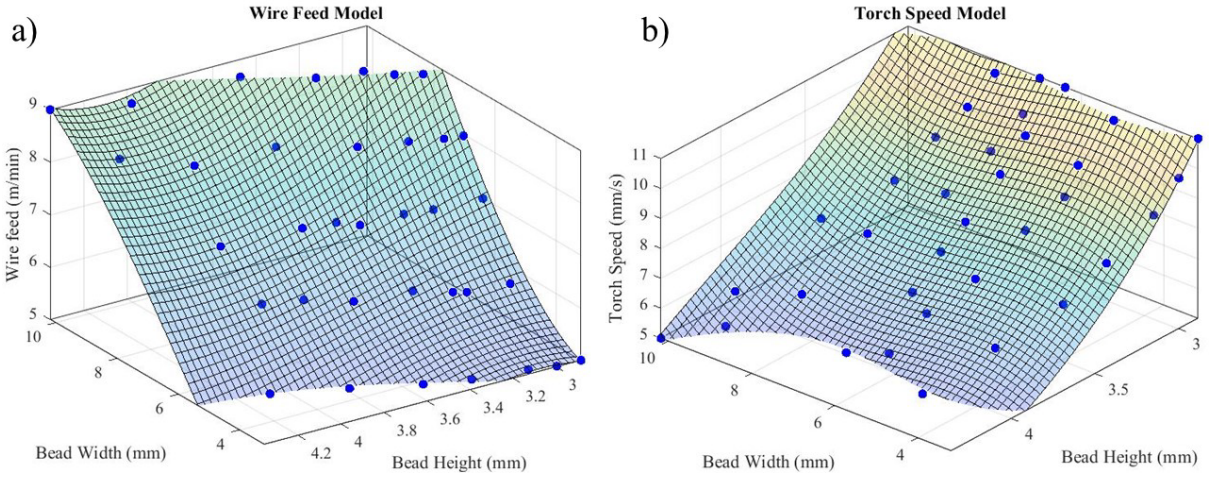

Fig. 7: process parameter model for a) wire feed and b) torch speed with respect to bead width and height

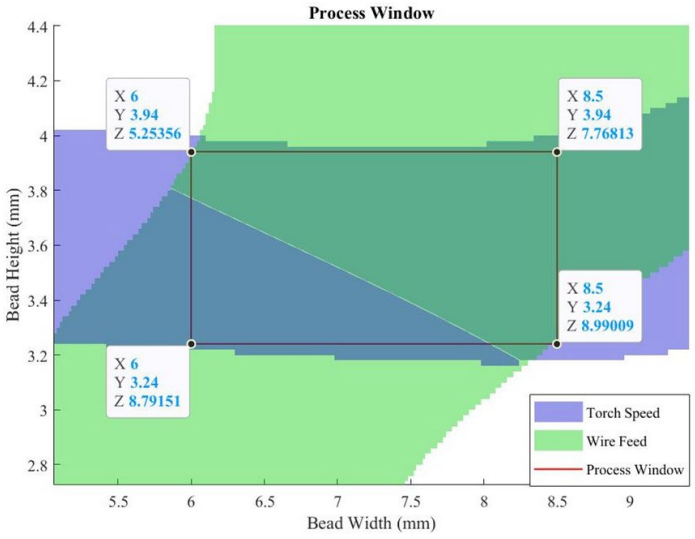

Fig. 8: Process window chosen for nickel aluminium bronze, green is the wire feed model, blue is the torch speed model

Based on the bead dataset, a polynomial surface of degree 3 was chosen for Eqn. 2, and its fit is as shown in Fig. 7. The torch speed and wire feed model found experimentally was found to be Eqn. 4 And Eqn. 5 respectively, where x refers to the desired bead width and y refers to the desired bead height.

$$v_{torch} = 85.74 + 3.456x - 55.13y - 0.7515x^2 + 0.5753xy + 11.71y^2 + 0.02981x^3 + 0.05171x^2y - 0.162xy^2 - 0.8327y^3 \quad (4)$$

$$v_{wire} = -38.05 + 2.767x + 33.08y + 0.4632x^2 - 2.771xy - 7.412y^2 - 0.006967x^3 - 0.08017x^2y + 0.5094xy^2 + 0.4294y^3 \quad (5)$$

Notice that from the plot, the bead width seems mainly influenced by wire feed, while the bead height is largely affected by torch speed. Based on the obtained process map, a rectangular process window was chosen with a wire feed of at least 5.8m/min and a torch speed of at least 0.54 m/min to control the correction process. The choice to sacrifice wire feed speed below 5.8 m/min and torch speed above 0.54 m/min was to balance the reduction in bead width or height correction range when going beyond these limits. Fig.8 shows the resulting achievable bead printable ranges based on the chosen wire feed speed and torch speed limits, as demarked in green and blue, respectively. That is, a bead width between 6mm to 8.5mm and a bead height between 3.24mm to 3.94mm.

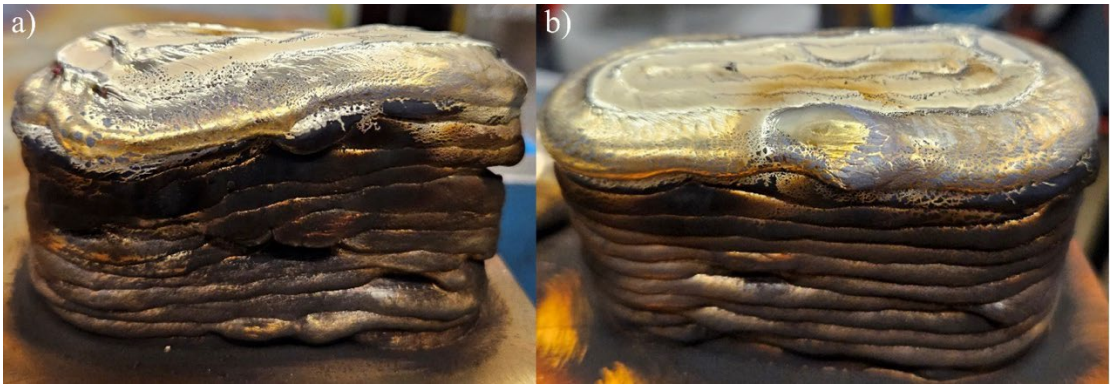

Fig. 9: Example part printed with a) Constant height b) Variable height

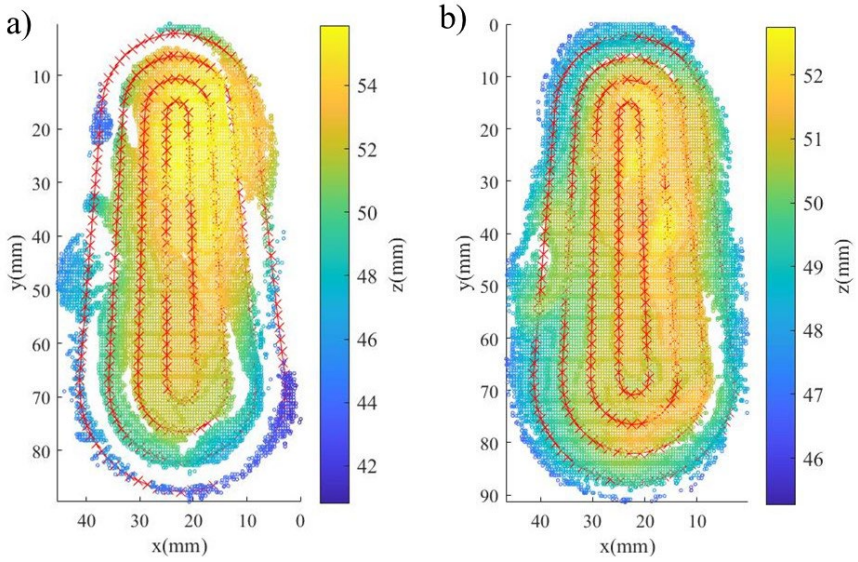

Fig. 10: Surface scan of geometry after 13 layers with a) constant height process b) variable height process

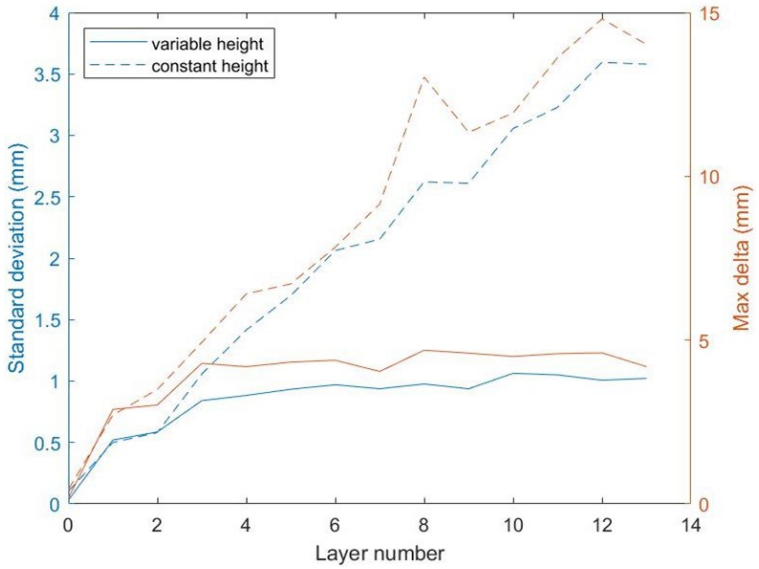

Fig. 11: Plot of standard deviation and maximum delta to layer number and a fitted line of constant height max delta in green

To test the proposed height correction framework, 13 layers of the rounded bar geometry were printed with and without height correction up to a final height of about 50mm. As shown in Fig. 9, the results show that the use of a height correction process showed a marked improvement in the top surface flatness. To quantify the error build-up at each layer, we sampled the print height at each toolpath point by superimposing the toolpath of the layer onto the height profile with an example of layer 13 as shown in Fig. 10 For each layer of each part, we computed its standard deviation and maximum delta within the layer's sampled points and plotted it, as shown in Fig. 11. Notice that the first two layers show little difference between with and without correction control and this can be attributed to the feedback nature of the variable height process where compensation depends on the presence of error. However, this is not the case from the third layer onwards, where the error accumulation grows but stabilizes quickly with the implementation of a height correction process. This verifies the feasibility of our proposed height correction approach.

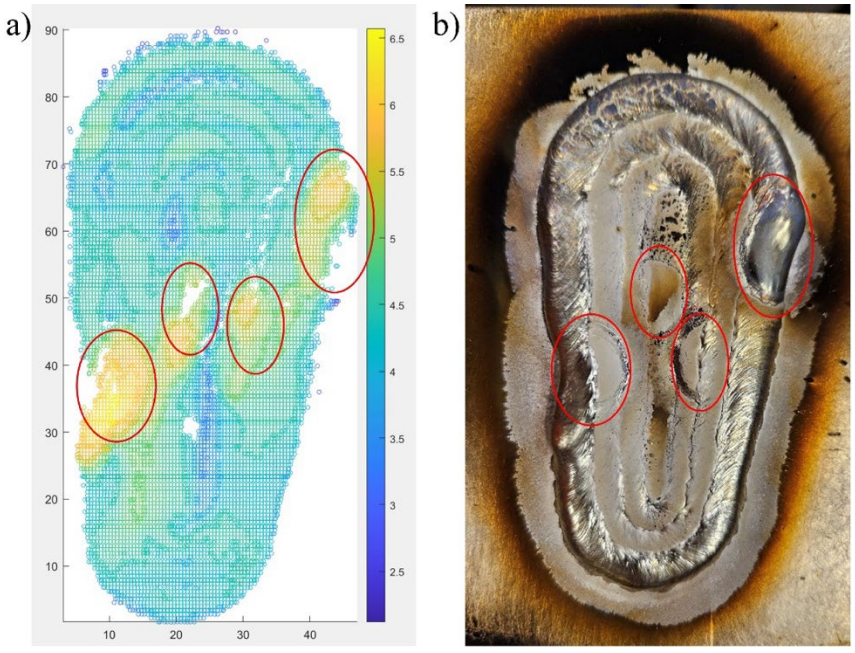

Fig. 12: a) Height profile scan b) Photo of first layer with start stop regions circled with red

From the results, it is interesting to note that the standard deviation of the first layer is 0.52mm while the maximum deviation reaches 2.88mm, much larger than the 0.7 mm adjustable height range. The tall regions in Fig.12a coincide with the peaks seen at the start-stop regions, as circled in red in Fig.12b. These contribute to the extreme deviation within a layer. Recall that the inconsistency of the bead at the start-stop is also discussed in [4] and is expected in WAAM. To mitigate this issue, one strategy was to shift the start-stop region across the layers, spreading the error and allowing correction to be performed across multiple layers, reducing the height correction range requirement.

Conclusion

Through the sample part, we have verified the feasibility of an in-situ print height correction approach to stabilize height variation to within 5mm instead of 15mm over multiple layers. The approach utilized a regression-based process model to provide suitable process parameters to achieve the target bead width and height. This enables printing of taller parts potentially into hundreds of layers while ensuring consistent print height to minimize print failure of large components which are ideal for WAAM. The potential to eliminate the need for intervention strategies is beneficial to reduce time and material usage while also reducing equipment cost for intervention process. However, it is noted that even though the experiments showed promising results, there is a limit to the range of height errors it can correct. As part of future work, different print conditions, such as steeper overhangs, varying toolpaths, and different materials, will be conducted to understand the limits of the correction process. In addition, different process window shapes other than rectangular could be explored to cater to different toolpaths or slicing requirements. This could further help optimize the process window for a particular toolpath to facilitate larger correction limits and, thus, error correction capability.

References

[1] S. Suryakumar, K. Karunakaran, A. Bernard, U. Chandrasekhar, N. Raghavender and D. Sharma, "Weld bead modeling and process optimization in Hybrid Layered Manufacturing," *Computer-Aided Design,* vol. 43, no. 4, pp. 331-344, 2011.

[2] D. Ding, Z. Pan, D. Cuiuri and H. Li, "A multi-bead overlapping model for robotic wire and arc additive manufacturing (WAAM)," *Robotics and Computer-Integrated Manufacturing,* vol. 31, pp. 101-110, 2015.

[3] X. Y. Oh and G. S. Soh, "Wire Arc Additive Manufacturing Stepover Optimization based on Varying-Ratio Flat-Top Overlapping Model," in *International Conference of Asian Society for Precision Engineering and Nanotechnology*, Singapore, 2022.

[4] Z. Hu, X. Qin, T. Shao and H. Liu, "Understanding and overcoming of abnormity at start and end of the weld bead in additive manufacturing with GMAW," *The International Journal of Advanced Manufacturing Technology,* vol. 95, no. 5, pp. 2357-2368, 2018.

[5] X. Wang, A. Wang and Y. Li, "A sequential path-planning methodology for wire and arc additive manufacturing based on a water-pouring rule," *The International Journal of Advanced Manufacturing Technology,* vol. 103, pp. 3813-3830, 2019.

[6] N. A. Rosli, M. R. Alkahari, F. R. Ramli and M. F. Abdollah, "Influence of process parameter on the height deviation of weld bead in wire arc additive manufacturing," *Int. J. Mech. Prod. Eng. Res. Dev,* vol. 10, no. 3, pp. 1165-1176, 2020.

[7] F. Youheng, W. Guilan, Z. Haiou and L. Liye, "Optimization of surface appearance for wire and arc additive manufacturing of Bainite steel," *The International Journal of Advanced Manufacturing Technology,* vol. 91, pp. 301-313, 2017.

[8] D. Ding, Z. Pan, D. Cuiuri, H. Li and N. Larkin, "Adaptive path planning for wire-feed additive manufacturing using medial axis transformation," *Journal of Cleaner Production,* vol. 133, pp. 942-952, 2016.

[9] Y. Xiong, S.-I. Park, S. Padmanathan, A. G. Dharmawan, S. Foong, D. W. Rosen and G. S. Soh, "Process planning for adaptive contour parallel toolpath in additive manufacturing with variable bead width," *The International Journal of Advanced Manufacturing Technology,* vol. 105, no. 10, pp. 4159-4170, 2019.

[10] T. F. Lam, Y. Xiong, A. G. Dharmawan, S. Foong and G. S. Soh, "Adaptive process control implementation of wire arc additive manufacturing for thin-walled components with overhang features," *The International Journal of Advanced Manufacturing Technology,* vol. 108, no. 4, pp. 1061--1071, 2020.

[11] Y. M. Elkhouly, W. S. Lim, A. G. Dharmawan and G. S. Soh, "Adaptive contour based printing of a propeller using hybrid-wire arc additive manufacturing," *Materials Today: Proceedings,* vol. 70, pp. 395-400, 2022.

[12] W. S. Lim, A. G. Dharmawan and G. S. Soh, "Development and performance evaluation of a hybrid-wire arc additive manufacturing system based on robot manipulators," *Materials Today: Proceedings,* vol. 70, pp. 587-592, 2022.

[13] Y. Li, X. Li, G. Zhang, I. Horváth and Q. Han, "Interlayer closed-loop control of forming geometries for wire and arc additive manufacturing based on fuzzy-logic inference," *Journal of Manufacturing Processes,* vol. 63, pp. 35-47, 2021.

[14] A. G. Dharmawan, Y. Xiong, S. Foong and G. S. Soh, " A Model-Based Reinforcement Learning and Correction Framework for Process Control of Robotic Wire Arc Additive Manufacturing," in *IEEE International Conference on Robotics and Automation (ICRA)*, Paris, 2020.